

## Laser (248 nm) Flash Photolysis and Pulse Radiolysis of CF<sub>2</sub>Br<sub>2</sub> in Aqueous Solution: Atmospheric Implications

Rameshwar D. Saini,\* Suresh Dhanya, and Tomi Nath Das

Radiation Chemistry & Chemical Dynamics Division, Bhabha Atomic Research Centre, Trombay, Mumbai - 400 085, India

(Received July 11, 2001)

Henry's law constant ( $K_h$ ) of CF<sub>2</sub>Br<sub>2</sub> was measured to be 0.058 M atm<sup>-1</sup> at room temperature. The steady state as well as laser (248 nm) flash photolysis of CF<sub>2</sub>Br<sub>2</sub> was carried out in aqueous solution. The formation of Br<sub>2</sub><sup>•-</sup> radicals involving two primary photodissociation channels was observed in the flash photolysis. One channel produced CF<sub>2</sub>Br<sup>•</sup> and Br<sup>•</sup> radicals, and the other led to the formation of Br<sup>-</sup> and H<sup>+</sup>. The spectrum and reactions of CF<sub>2</sub>Br<sup>•</sup> were studied in aqueous solution by pulse radiolysis. The CF<sub>2</sub>Br<sup>•</sup> radical was found to absorb in the 230–270 nm region with a molar absorbance ( $\epsilon$ ) of 710 M<sup>-1</sup> cm<sup>-1</sup> at  $\lambda_{\max}$  = 245 nm. The rate constants of some of the reactions were measured at 299 K as follows:  $k(e_{\text{aq}}^- + \text{CF}_2\text{Br}_2) = 1.20 \pm 0.13 \times 10^{10}$ ,  $2k(\text{CF}_2\text{Br}^\bullet + \text{CF}_2\text{Br}^\bullet) = 1.4 \pm 0.4 \times 10^9$ ,  $k(\text{CF}_2\text{Br}^\bullet + \text{O}_2) = 1.9 \pm 0.5 \times 10^9 \text{ M}^{-1} \text{ s}^{-1}$ . The CF<sub>2</sub>BrO<sub>2</sub><sup>•</sup> radical absorbed in the 245–360 nm region with  $\epsilon = 593 \text{ M}^{-1} \text{ cm}^{-1}$  at  $\lambda_{\max} = 265$  nm. An apparatus used to measure  $K_h$ , and a closed-loop flow system used to carry out the flash photolysis/pulse radiolysis of sparingly soluble gases, like CF<sub>2</sub>Br<sub>2</sub>, are reported.

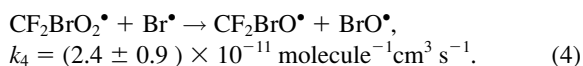
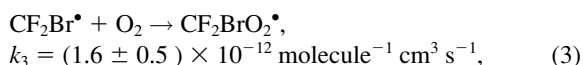
There is continuing interest in the UV photodissociation dynamics of CF<sub>2</sub>Br<sub>2</sub> (halon-1202) for two reasons: 1) an understanding of the dissociative pathways of simple molecules like CF<sub>2</sub>Br<sub>2</sub> is of fundamental importance,<sup>1</sup> 2) CF<sub>2</sub>Br<sub>2</sub> belongs to a family of halomethanes, whose ultraviolet photodissociation in the stratosphere initiates the well-known ozone-depletion cycle<sup>2,3</sup> involving ClO<sup>•</sup> and BrO<sup>•</sup> radicals; although its concentration in the atmosphere has been found to be increasing over the past few years, it is not covered by the Montreal Protocol.<sup>4,5</sup> The photodissociation dynamics has been studied experimentally using a wide variety of methods and wavelengths ranging from 223 nm to 260 nm,<sup>6–12</sup> as well as theoretically.<sup>13</sup> The primary step has been identified as



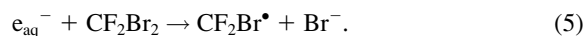
with a quantum yield of almost unity.<sup>6,14</sup> In addition, it has been observed that about 16% of the CF<sub>2</sub>Br<sup>•</sup> radical produced by reaction (1) has sufficient energy to spontaneously dissociate into the <sup>•</sup>CF<sub>2</sub> radical and the Br atom<sup>8,11,12</sup>, i.e.



Also, Dhanya et al., using 248 nm laser flash photolysis, have shown the formation of the BrO<sup>•</sup> radical by the following route:<sup>15</sup>



However, to our knowledge, all studies on the ultraviolet photodissociation of CF<sub>2</sub>Br<sub>2</sub> have so far been carried out in the gas phase, and no attempt has been made to investigate the photochemistry of CF<sub>2</sub>Br<sub>2</sub> in the condensed aqueous phase, which remains present in the atmosphere in the form of clouds, fog, rain, dew, and wet aerosol particles, so much so that clouds cover approximately 60% of the Earth's surface.<sup>3</sup> Any gaseous species released into the atmosphere has to distribute itself between the gaseous phase and the condensed aqueous phase; our experiments show that CF<sub>2</sub>Br<sub>2</sub> is not an exception to this rule. Upon dissolution in a condensed aqueous phase, the subsequent thermal or photochemistry of a chemical species is expected to be quite different, not only due to subsequent favorable energetics for newer reaction pathways, but also due to the possibility of self-ionization, pH or ionic effects and the enhanced concentration and proximity to other reactive species, e.g., dissolved O<sub>2</sub>.<sup>16</sup> Further, it is now well known that heterogeneous reactions on the surfaces of polar stratospheric clouds play a pivotal role in the formation of the ozone hole.<sup>3,17</sup> We have therefore measured the Henry's law coefficient ( $K_h$ )<sup>18</sup> of CF<sub>2</sub>Br<sub>2</sub>, and checked the effect of UV-light on its aqueous chemistry, both under steady state conditions using a low-pressure Hg-lamp as well as with 248 nm laser flash photolysis. Due to the complex chemistry observed in the presence of UV light, *e*-beam pulse radiolysis studies were also undertaken to study the properties of the primary photodissociation product, CF<sub>2</sub>Br<sup>•</sup>. In this case, the CF<sub>2</sub>Br<sup>•</sup> radical could be generated by the well-known dissociative electron-capture reaction of halocarbons,<sup>19</sup> reaction (5), without any interference from other species (like Br<sup>•</sup> and <sup>•</sup>CF<sub>2</sub> radical transients), thereby allowing the measurement of its UV absorption spectrum and also some relevant reaction kinetics,



The  $\text{CF}_2\text{Br}_2^-$  type radical formed after electron capture has not been reported in measurements on the  $\mu\text{s}$  time scale. Instead, concurrent dehalogenation takes place in solution; in this case bromine is preferentially released over fluorine. A closed-loop continuous flow system was designed to maintain the desired concentration of dissolved  $\text{CF}_2\text{Br}_2$  and other reactants during the course of the study.

### Experimental

**General.** All experiments were carried out at an ambient temperature of 299 K unless otherwise stated. Triply distilled water was used to prepare all aqueous solutions, where distilled water was further distilled over (a) acidic dichromate and (b) alkaline permanganate. The gases and chemicals were of reagent grade. Atmospheric air was purified by passing through a column of freshly activated charcoal, and  $\text{CF}_2\text{Br}_2$  from Aldrich (> 97%) was degassed before use. A grease-free vacuum setup for attaining a vacuum of  $1 \times 10^{-3}$  Torr was used when required. All pressure measurements were made with capacitance manometers (MKS Baratrons, Type 122A), and the absorption spectra were recorded using a Hitachi-330 spectrophotometer.

**Determination of Henry's Law Constant of  $\text{CF}_2\text{Br}_2$ .** Measurements of  $K_h$  were carried out using the apparatus schematically shown in Fig. 1. In principle, our method involved measuring the concentration of gaseous  $\text{CF}_2\text{Br}_2$  spectrophotometrically in cuvette B, before and after equilibration with a known quantity of degassed water contained in cuvette A. We carried out spectrophotometric measurements on a number of gas mixtures, each containing 21 Torr of water vapor in the presence of  $\text{CF}_2\text{Br}_2$  with its partial pressure ranging from 1 to 15 Torr. We found that the presence of water vapor did not have any effect on the absorption spectrum and the absorption cross section ( $\sigma$ ) of gaseous  $\text{CF}_2\text{Br}_2$ . Hence, the reported values of the absorption cross section ( $\sigma$ ) of  $\text{CF}_2\text{Br}_2$  at different wavelengths<sup>20</sup> in the gas phase were used to

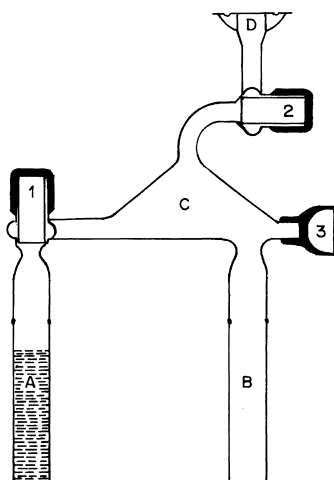


Fig. 1. Apparatus for determining the Henry's law constant ( $K_h$ ) (schematic). A and B: Far UV Grade spectrophotometric cuvettes of 10 mm path length, A for liquid and B for gas; C: equilibration chamber; 1, 2: Grease free high vacuum stopcocks; 3: sampling port with viton/silicone rubber septum for gas chromatographic analysis; D: O-ring connector.

calculate the exact partial pressure.

The preparation as well as the handling of the aqueous solutions was carried out in a closed-loop system using the apparatus shown in Fig. 2. Briefly, a solution of known composition was prepared in flask A, and flowed through reaction cell C; the spent solution was collected in flask D. Reaction cell C was made from a Suprasil<sup>TM</sup> tube of 1 cm  $\times$  1 cm square bore. All operations were carried out at sub-atmospheric pressures and in an air-free environment, unless otherwise stated.

**UV Photolysis.** Steady-state photolysis was carried out in a stoppered cuvette using a Pen-Ray low-pressure mercury lamp. Another cuvette containing methanol was placed between the lamp and the sample to cut off the mercury lines of  $\lambda \leq 184.9$  nm. The experimental setup for the KrF (248 nm) laser flash photolysis was described earlier.<sup>15</sup> The laser intensity was measured with respect to the yield of biphenyl triplet using an oxygen-free solution of biphenyl in cyclohexane having an absorbance equal to that of the experimental solution of  $\text{CF}_2\text{Br}_2$  at 248 nm. The values for the quantum yield and the molar absorbance of the biphenyl triplet were taken as 0.84 and  $4.28 \times 10^4 \text{ M}^{-1} \text{ cm}^{-1}$ , respectively.<sup>21</sup> The maximum laser intensity was  $1.74 \times 10^{16} \text{ photon cm}^{-2}$ , and it was varied by placing several flat plates of technical-grade quartz, each having a transmission of about 85% at 248 nm.

**Pulse Radiolysis Setup.** Pulse radiolysis studies were carried out using an experimental setup described earlier.<sup>22,23</sup> Briefly, the solution was exposed to an electron pulse from a linear accelerator

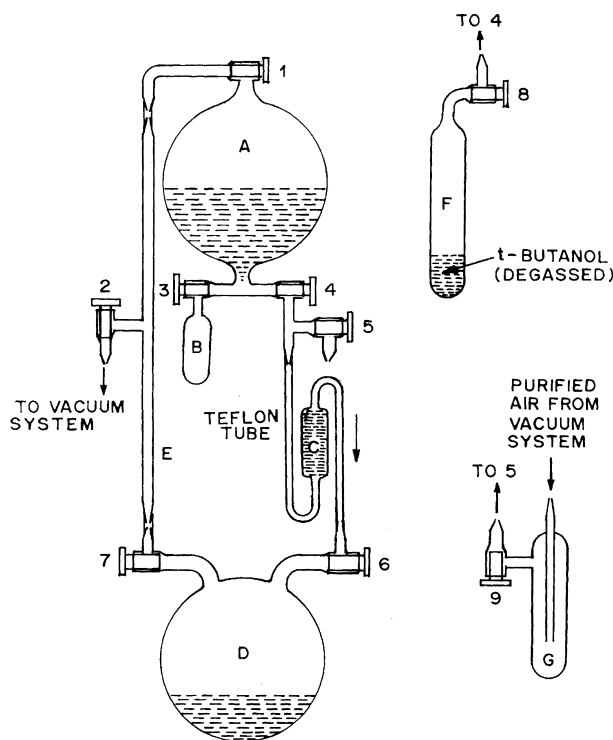


Fig. 2. Apparatus for the preparation and manipulation of aqueous solutions of  $\text{CF}_2\text{Br}_2$  for pulse radiolysis (schematic). A: Reservoir for the preparation and storage of feed solution, total capacity = 0.6 L.; B: Ampoule to store the measured amount of  $\text{CF}_2\text{Br}_2$  before mixing; C: Flow cell for pulse radiolysis, made from Suprasil tube of 10 mm  $\times$  10 mm internal cross section, D: Receiver; 1-9: Grease free high vacuum stopcocks.

(Forward Industries, UK) and the transient species were monitored by kinetic spectrophotometry. The linear accelerator provided pulses of 7 MeV electrons with a duration that could be varied between 50 ns and 2  $\mu$ s with a corresponding dose range of  $\sim 3$  Gy to 140 Gy, respectively. The dosimetry was carried out with an aerated aqueous solution containing  $10^{-2}$  M potassium thiocyanate, while taking into account that  $G \cdot \epsilon = 2.59 \times 10^{-4} \text{ m}^2 \text{ J}^{-1}$  at 475 nm.<sup>24</sup> The interference due to the scattered light at 250 nm was  $< 2\%$ , measured by comparing the transmitted light intensity with and without a Pyrex filter. The spectral measurements were made at a wavelength resolution of about 2.5 nm.

### Results and Discussion

**Behavior of  $\text{CF}_2\text{Br}_2$  in Aqueous Solution.** The addition of  $\text{CF}_2\text{Br}_2$  did not change the pH of water, and a saturated aqueous solution of  $\text{CF}_2\text{Br}_2$  did not produce any precipitate upon the addition of  $\text{AgNO}_3$ , even after keeping for several days in the dark. These observations rule out the occurrence of the hydrolytic reaction (6), i.e.,



The absorption spectrum of  $\text{CF}_2\text{Br}_2$  in the gas and aqueous phases are shown in Fig. 3. The  $\lambda_{\text{max}}$  of  $\text{CF}_2\text{Br}_2$  in the aqueous solution was blue shifted by 3 nm compared to that in the gas phase; this is expected from the solvent effect on the  $n-\sigma^*$  transition involved.<sup>25</sup> In addition, it was also found that the intensity of absorption is higher in the gas phase than in solution. A similar solvent effect on the absorption characteristics of a molecule, undergoing  $n-\sigma^*$  transition was observed earlier, e.g., in dimethyl sulfide.<sup>26,27</sup>

**Henry's Law Constant ( $K_h$ ) of  $\text{CF}_2\text{Br}_2$ .** From repeated

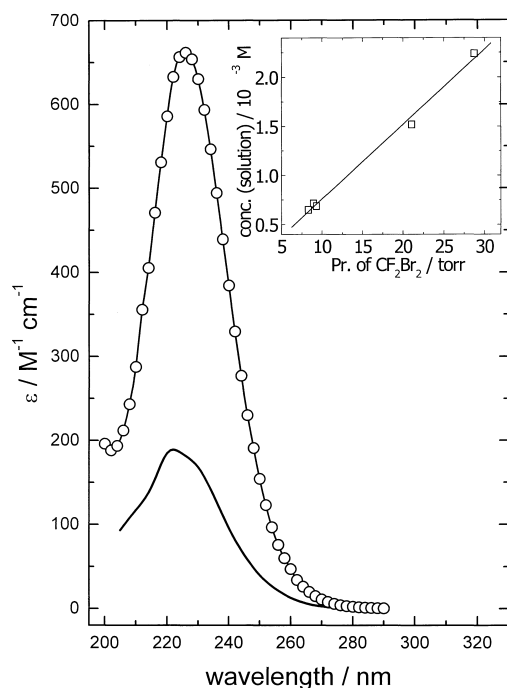


Fig. 3. Absorption spectra of  $\text{CF}_2\text{Br}_2$  in gas phase ( $\circ$ ) and aqueous solution ( $—$ ). Inset: Measurement of Henry's law constant ( $K_h$ ).

measurements under the conditions employed (Fig. 3 Inset), the value of  $K_h$  was determined to be  $0.058 \text{ M atm}^{-1}$  at 299 K.

**UV Photolysis.** The laser (248 nm) flash photolysis of an air-free aqueous solution containing  $6.7 \times 10^{-3}$  M of  $\text{CF}_2\text{Br}_2$  yielded a transient absorption spectrum with an absorption maximum ( $\lambda_{\text{max}}$ ) at  $\sim 360$  nm, as shown in Fig. 4. The absorption at 360 nm decayed by second-order kinetics with  $2k/\epsilon l = 6.14 \pm 0.40 \times 10^5 \text{ s}^{-1}$ . The formation of the transient species was found to be quite fast, and attained its peak absorbance value within about 2  $\mu$ s after the laser pulse. A log-log plot (Fig. 4 inset) between the peak absorbance ( $\Delta A$ ) and the laser intensity ( $I$ ) gives a slope of 2, thereby indicating the involvement of two photons in its generation. The bubbling of atmospheric air into the experimental solution had practically no effect on the intensity and the decay kinetics of transient absorption at 360 nm. Upon steady state photolysis for a period of 5 minutes with the  $\lambda \geq 235$  nm light, another portion of the same solution showed the following changes: a) it acquired a brown tinge, b) its pH changed from 5.8 to 2.5, and c) it gave a precipitate of  $\text{AgBr}$  upon the addition of a solution of  $\text{AgNO}_3$ . Similar changes were observed on exposing the solution to about 500 flashes of a 248 nm laser.

### Pulse Radiolysis. Transient Absorption Spectrum.

The radiolysis of water at pH 7 leads to the formation of primary radicals,  $e_{\text{aq}}^-$ ,  $\text{H}^\bullet$ , (both reducing) and  $\bullet\text{OH}$  (oxidizing) with respective yields of 0.28, 0.062, and  $0.28 \mu\text{mol J}^{-1}$ .<sup>28</sup> The transient absorption spectrum shown in Fig. 5(a) was obtained from the pulse radiolysis of an air-free aqueous solution containing  $1.4 \times 10^{-3}$  M of  $\text{CF}_2\text{Br}_2$ ; it shows two absorption maxima ( $\lambda_{\text{max}}$ ) at  $\sim 240$  nm and  $\sim 350$  nm. From kinetic measurements at these two wavelengths, the formation and decay rates

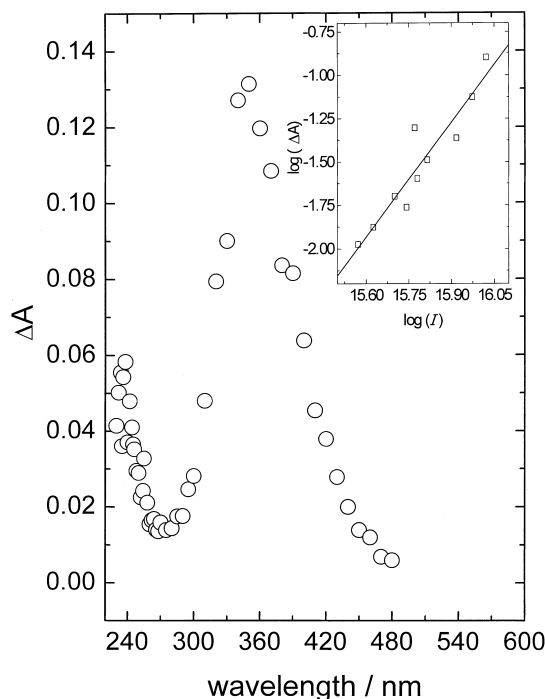


Fig. 4. Transient absorption spectrum, 3  $\mu$ s after 248-nm laser flash.  $[\text{CF}_2\text{Br}_2] = 6.7 \times 10^{-3}$  M. Inset: Dependence of peak absorbance (360 nm) on laser intensity.

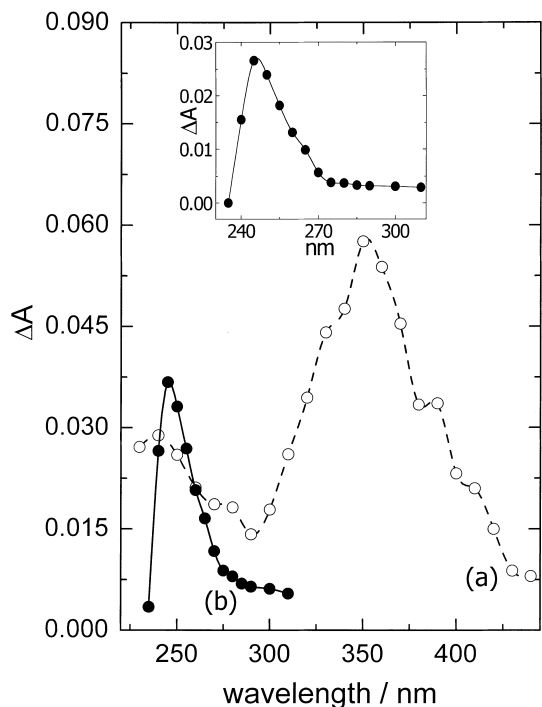
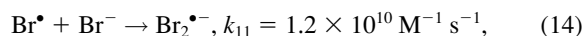
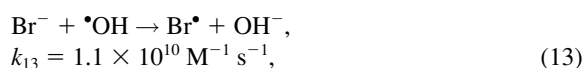
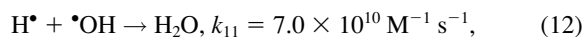
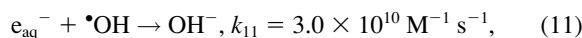
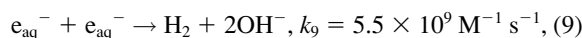
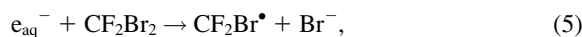
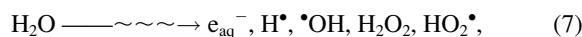


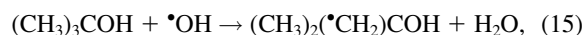
Fig. 5. Transient absorption spectra at the end of 2  $\mu$ s pulse. (a)  $[\text{CF}_2\text{Br}_2] = 1.4 \times 10^{-3}$  M, (b)  $[\text{CF}_2\text{Br}_2] = 1.4 \times 10^{-3}$  M;  $[\text{1,1-dimethylethanol}] = 0.2$  M. Inset: spectrum (b) after correction for the depletion of  $\text{CF}_2\text{Br}_2$  and for the absorption due to 1,1-dimethylethanol radical; dose = 108 Gy.

were found to be quite different from each other, thus suggesting the formation of two different species. A comparison revealed that the transient absorption with  $\lambda_{\text{max}}$  at  $\sim 350$  nm resembles that reported for  $\text{Br}_2^{\bullet-}$  in the literature.<sup>29</sup> Accordingly, the above results can be explained by the following set of reactions:<sup>19</sup>



and the transient absorption with  $\lambda_{\text{max}}$  at 240 nm can be assigned to the  $\text{CF}_2\text{Br}^\bullet$  radical. The growth rate at  $\sim 350$  nm has

been found to be dose dependent, as would be expected from the above reaction scheme. For example, with a 2  $\mu$ s pulse (dose = 108 Gy), the peak absorption was reached within the duration of the pulse, whereas with a 500 ns pulse (dose = 56 Gy) it took as much as 21  $\mu$ s to attain the peak-absorbance at 350 nm. The above mechanism is further supported by a similar experiment in the presence of 0.2 M 1,1-dimethylethanol (2-Methyl-2-propanol), wherein the transient absorption with  $\lambda_{\text{max}}$  at 350 nm disappeared completely, and the one with  $\lambda_{\text{max}}$  at 240 nm became modified [Fig. 5b]. This is due to the fact that reaction (13) is suppressed by the following reaction:



and the resultant  $\beta$ -hydroxy radical,  $(\text{CH}_3)_2(\bullet\text{CH}_2)\text{COH}$ , absorbs in the 220–300 nm<sup>30</sup> region. Upon subtracting the contribution of the  $(\text{CH}_3)_2(\bullet\text{CH}_2)\text{COH}$  radical, and making a correction for the loss of absorption due to depletion of the parent compound,  $\text{CF}_2\text{Br}_2$ , (using spectrum in Fig. 3), we obtained the corrected absorption spectrum of  $\text{CF}_2\text{Br}^\bullet$  radical, as shown in Fig. 5 (Inset).

#### Rate Constant for the Reaction of $e_{\text{aq}}^-$ with $\text{CF}_2\text{Br}_2$

The kinetics of hydrated electron decay, monitored at 720 nm, was found to become faster in the presence of  $\text{CF}_2\text{Br}_2$ , as shown in Fig. 6. The observed rate constant of  $e_{\text{aq}}^-$  decay increases with increasing concentration of  $\text{CF}_2\text{Br}_2$  from 1 to 6  $\times 10^{-4}$  M, as shown in Fig. 6 (Inset). From the slope of this plot, the bimolecular rate constant for reaction (5) was calculated to be  $(1.20 \pm 0.13) \times 10^{10} \text{ M}^{-1} \text{ s}^{-1}$ . An attempt to crosscheck

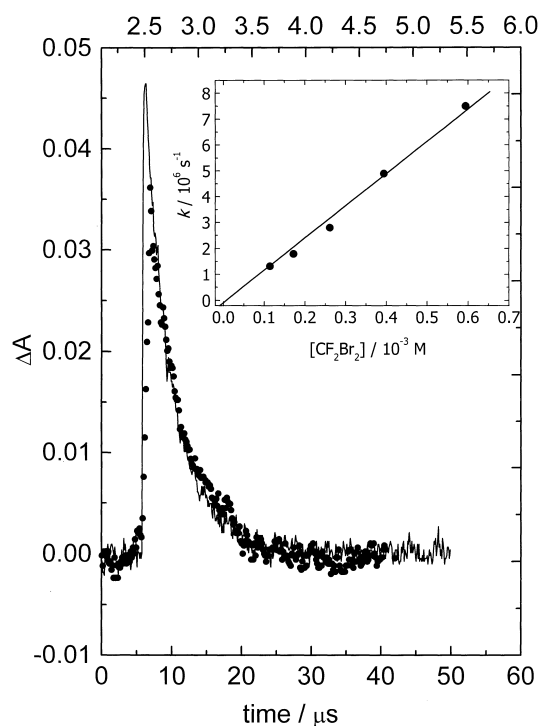


Fig. 6. Decay of  $e_{\text{aq}}^-$  at 720 nm in blank matrix (—) (bottom x-axis) and in the presence of  $2.6 \times 10^{-4}$  M  $\text{CF}_2\text{Br}_2$  (●) (top x-axis); 50 ns pulse; dose = 12 Gy. Inset: Dependence of observed rate constant on  $\text{CF}_2\text{Br}_2$  concentration.

the value of  $k_5$  by observing the growth rate of  $\text{CF}_2\text{Br}^\bullet$  at  $\sim 250$  nm was unsuccessful, because the signal was weak and had interfering optical absorption from the following: a) the parent compound (bleaching), b)  $\text{e}_{\text{aq}}^-$  and c) the  $(\text{CH}_3)_2(\bullet\text{CH}_2)\text{COH}$  radical in the presence of 1,1-dimethylethanol.

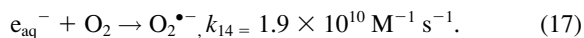
**Molar Absorbance and Decay Kinetics of  $\text{CF}_2\text{Br}^\bullet$  Radical.** From the rate constants of competing reactions (5), (9), and (11), it follows that  $> 97\%$  of hydrated electron is consumed by reaction (5) in the presence of  $1.4 \times 10^{-3}$  M  $\text{CF}_2\text{Br}_2$ . Thus,  $G(\text{CF}_2\text{Br}^\bullet) = 0.97 \times G(\text{e}_{\text{aq}}^-)$ , where the effects of reaction (8), and any reaction of  $\text{CF}_2\text{Br}^\bullet$  radical within this time period, are neglected. Using the values of the radiolytic yield of  $\text{e}_{\text{aq}}^-$  and the radiation dose absorbed (108 Gy), in a typical set of experiments, we calculated the initial concentration of  $\text{e}_{\text{aq}}^- = 3.7 \times 10^{-5}$  M and that of  $\text{CF}_2\text{Br}^\bullet$  radical  $= 3.6 \times 10^{-5}$  M, which led to the molar absorbance of  $\text{CF}_2\text{Br}^\bullet$  radical at  $\lambda_{\text{max}}$ , 245 nm  $= 710 \text{ M}^{-1} \text{ cm}^{-1}$ . By considering the slopes of  $1/\Delta A$  vs time plot and  $\epsilon$  at 260, 265, and 270 nm, where absorption due to the parent compound is negligible, we obtained an average value of  $1.4 \pm 0.4 \times 10^9 \text{ M}^{-1} \text{ s}^{-1}$  ( $2k$ ) for the rate constant of the bimolecular decay of  $\text{CF}_2\text{Br}^\bullet$  radical.

**Reaction of  $\text{CF}_2\text{Br}^\bullet$  Radical with  $\text{O}_2$ .** Using an aqueous solution containing  $3 \times 10^{-3}$  M  $\text{CF}_2\text{Br}_2$  and varying the concentration of oxygen from  $10^{-5}$  to  $10^{-4}$  M, the following reaction was studied:



The decay of the  $\text{CF}_2\text{Br}^\bullet$  radical was monitored at 250 nm, and was found to follow a pseudo first-order kinetics, giving the product  $\text{CF}_2\text{BrO}_2^\bullet$  radical within 30–8  $\mu\text{s}$  for  $\text{O}_2$  concentrations ranging over 25–125  $\mu\text{M}$ . From a plot of the observed rate constants against the concentration of oxygen (Fig. 7, Inset), the bimolecular rate constant of reaction (16) was calculated to be  $(1.9 \pm 0.5) \times 10^9 \text{ M}^{-1} \text{ s}^{-1}$ .

**Absorption Spectrum of  $\text{CF}_2\text{BrO}_2^\bullet$  Radical.** The absorption spectrum of the peroxy radical,  $\text{CF}_2\text{BrO}_2^\bullet$ , is shown in Fig. 7. This was obtained by the pulse radiolysis of an air-equilibrated aqueous solution containing  $1.55 \times 10^{-2}$  M  $\text{CF}_2\text{Br}_2$ , and  $2.7 \times 10^{-4}$  M oxygen,<sup>21</sup> using a dose of 56 Gy. Under these conditions, the following reaction is almost completely suppressed by reaction (5), thereby minimizing the interference due to  $\text{O}_2^{\bullet-}$  radical, which also absorbs in the 240–280 nm region:



Also, the interference from  $\text{Br}_2^{\bullet-}$  radical is negligible because of its slow formation, taking about 21  $\mu\text{s}$ , at the dose employed. The spectrum (Fig. 7), obtained at 0.7  $\mu\text{s}$  and corrected for the bleaching of  $\text{CF}_2\text{Br}_2$ , has  $\lambda_{\text{max}}$  at 265 nm, and it is quite different from that of the  $\text{CF}_2\text{Br}^\bullet$  radical (Fig. 5, Inset). Taking  $G(\text{CF}_2\text{BrO}_2^\bullet) \approx G(\text{CF}_2\text{Br}^\bullet)$ , the molar absorbance for  $\text{CF}_2\text{BrO}_2^\bullet$  radical was determined to be  $593 \text{ M}^{-1} \text{ cm}^{-1}$  at 265 nm.

The aim of the present work was to measure Henry's law constant ( $K_{\text{h}}$ ) of  $\text{CF}_2\text{Br}_2$  and to investigate the photochemistry of the latter in aqueous solution. Our measured value of  $K_{\text{h}}$  at 299 K indicates the solubility of  $\text{CF}_2\text{Br}_2$  in water under 1 atmo-

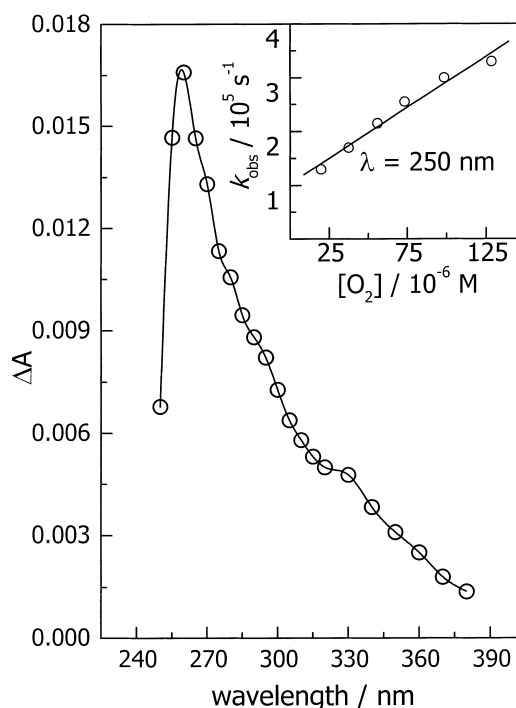


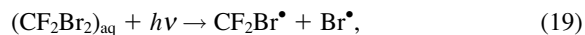
Fig. 7. Absorption spectrum of  $\text{CF}_2\text{BrO}_2^\bullet$  radical at 0.7  $\mu\text{s}$  after the 500 ns electron pulse.  $[\text{CF}_2\text{Br}_2] = 1.55 \times 10^{-2}$  M;  $[\text{O}_2] = 2.7 \times 10^{-4}$  M; dose = 56 Gy. Inset: Dependence of observed rate constant of  $\text{CF}_2\text{Br}^\bullet$  radical decay on the concentration of oxygen.

sphere pressure of the gas as  $5.78 \times 10^{-2}$  M. This is much higher than the reported solubilities of  $\text{CF}_3\text{Br}$  and  $\text{CFBr}_3$ , viz.,  $2.16 \times 10^{-3}$  and  $1.47 \times 10^{-3} \text{ M atm}^{-1}$ , respectively.<sup>31</sup> However, such large differences in the solubilities/Henry's law constants are not uncommon for such halocarbons, e.g., the values of  $K_{\text{h}}$  for  $\text{CCl}_2\text{F}_2$  and  $\text{CCl}_4$  are  $2.47 \times 10^{-3}$  and  $3.39 \times 10^{-2} \text{ M atm}^{-1}$ , respectively.<sup>31</sup> It may be pointed out that Henry's law constant and the solubility reported here correspond to the specific conditions of our experimental setup, where a gas is equilibrated with an aqueous solution over a flat surface. These results cannot be directly applied to the largely spherical or curved surfaces of atmospheric aerosols, which lead to a lowering of the solubility due to the Kelvin effect.<sup>3</sup> Further, the boiling point of  $\text{CF}_2\text{Br}_2$  (295 K) is very close to room temperature, and its specific gravity in the liquid phase is 2.271. Therefore, an attempt to measure the solubility by shaking the liquid  $\text{CF}_2\text{Br}_2$  with water and then allowing the aqueous and organic layers to separate out would result in a solubility higher than  $5.78 \times 10^{-2}$  M at room temperature, due to the fact that both liquid–liquid and liquid–gas equilibria would be simultaneously operative; the former at the lower interface and the latter at the upper one.

It is found that the absorption spectrum between 275 and 475 nm obtained after laser flash photolysis (Fig. 4) is very similar to that obtained by pulse radiolysis (Fig. 5a), which is assigned to the  $\text{Br}_2^{\bullet-}$  radical. This could form by a direct two-photon process, viz.,



However, reaction (18) cannot explain the formation of Br<sup>-</sup> in steady state photolysis, where the probability of its occurrence would be practically zero. Also, a biphotonic process involving the photoionization of CF<sub>2</sub>Br<sub>2</sub> molecule is not considered for the same reason. A plausible mechanism can be as follows:



where reactions (19) and (20) are two different primary photochemical reactions which generate the reactants Br<sup>•</sup> and Br<sup>-</sup> for reaction (14), and thus explain the intensity-square dependence of the formation of Br<sub>2</sub><sup>-</sup>. The photo-induced hydrolytic reaction (20) accounts for the lowering of the pH as well as for the formation of Br<sup>-</sup>. Further, reaction (19) represents a homolytic cleavage (giving radicals), which is favored in the gas phase as well as in non-polar solvents. Reaction (20) can be considered to involve a heterolytic cleavage (giving cation and anion), which is favored in polar solvents, like water, followed by the reactions of ionic fragments with the solvent-molecules available in the immediate vicinity, i.e.,



Since reaction (19) is a well-established primary photochemical reaction in the gas phase, the energy of the 248 nm photon (5 eV) is sufficient to overcome its activation barrier. On the other hand, the additional energy to overcome the extra high activation barrier of reaction (20) comes from the hydration energies of the final products, mainly those of the H<sup>+</sup> and Br<sup>-</sup> ions.

In addition, another difference in the photodissociation process taking place in solution can be from the 'cage effect', i.e., from a significant possibility that the surrounding water molecules would impede separation of the photofragments, and would thereby force some of them to undergo geminate recombination. However, experiments with a time resolution of pico or sub pico second resolution are required for a detail understanding of the formation of Br<sub>2</sub><sup>•-</sup>.

The formation of brown tinge (Br<sub>2</sub>/Br<sub>3</sub><sup>-</sup>) in steady state photolysis is possible by the following reactions:



From the above discussion, it follows that the transient absorption between 225 and 275 nm (Fig. 4) is likely to have contributions from more than one chemical species. Hence, we have used the pulse radiolysis technique to obtain reliable informa-

tion about the absorption spectrum and the reactivity of the primary product CF<sub>2</sub>Br<sup>•</sup> radical.

It has been estimated that on a per atom basis, bromine is ~50 times more efficient than chlorine in destroying atmospheric ozone.<sup>32</sup> This efficiency results from the fact that nearly 50% of the available bromine in the stratosphere exists in the reactive form (Br<sup>•</sup> and BrO<sup>•</sup>), whereas only a percent or so of stratospheric chlorine exists as ClO<sup>•</sup>. In view of this, it is interesting to examine the atmospheric implications of our results. A higher value of its solubility compared to that of most other halons and CFCs implies a reduced tropospheric lifetime for CF<sub>2</sub>Br<sub>2</sub> due to uptake by water in the oceans, rivers, lakes, etc. However, detail information on the marine chemistry of CF<sub>2</sub>Br<sub>2</sub> is required to understand whether the oceans act as a sink or reservoir for this molecule. In addition, an enhancement in the solubility of CF<sub>2</sub>Br<sub>2</sub> in the condensed aqueous phase at the lower temperatures encountered in the stratosphere may be significant. This possibility coupled with the fact that the UV photochemistry of CF<sub>2</sub>Br<sub>2</sub> in the aqueous phase is also different from that in the gas phase, partly leading to the formation of Br<sup>-</sup> and H<sub>3</sub>O<sup>+</sup> ions and hence to the mineralization of bromine, indicate that the findings of the present work are likely to have an important impact on the atmospheric modeling of CF<sub>2</sub>Br<sub>2</sub> and on the depletion of ozone.

We thank Mr. Vijendra N. Rao and his colleagues for their technical help in pulse radiolysis work.

## References

- 1 S. R. Lin and Y. P. Lee, *J. Chem. Phys.*, **111**, 9233 (1999).
- 2 L. T. Molina and F. S. Rowland, *Nature*, **249**, 810 (1974).
- 3 J. H. Seinfeld and S. N. Pandis, "Atmospheric Chemistry and Physics," John Wiley & Sons, New York (1998).
- 4 P. J. Fraser, D. E. Oram, S. E. Reeves, S. A. Penkett, and A. McCulloh, *J. Geophys. Res.*, **104**, 15985 (1999).
- 5 "New Scientist," 12-September-1998, p. 12.
- 6 R. K. Talukdar, G. L. Vaghjani, and A. R. Ravishankara, *J. Chem. Phys.*, **96**, 8194 (1992).
- 7 D. Krajnovich, Z. Zhang, L. Butler, and Y. T. Lee, *J. Phys. Chem.*, **88**, 4561 (1984).
- 8 T. R. Gosnell, A. J. Taylor, and J. L. Lyman, *J. Chem. Phys.*, **94**, 5949 (1991).
- 9 J. Van Hoeymissen, W. Uten, and J. Peeters, *J. Chem. Phys. Lett.*, **226**, 159 (1994).
- 10 R. K. Vatsa, A. Kumar, P. D. Naik, K. V. S. Rama Rao, and J. P. Mittal, *Bull. Chem. Soc. Jpn.*, **68**, 2817 (1995).
- 11 M. R. Cameron, S. A. Johns, G. F. Metha, and S. H. Kable, *Phys. Chem. Chem. Phys.*, **2**, 2539 (2000).
- 12 M. S. Park, T. K. Kim, Y. K. Lee, H. R. Volpp, and J. Wolfrum, *J. Phys. Chem. A*, **105**, 5606 (2001).
- 13 M. R. Cameron and G. B. Bacskay, *J. Phys. Chem. A.*, **104**, 11212 (2000).
- 14 L. T. Molina and M. Molina, *J. Phys. Chem.*, **87**, 3456 (1983).
- 15 S. Dhanya, R. D. Saini, P. D. Naik, and R. K. Vatsa, *Chem. Phys. Lett.*, **318**, 125 (2000).
- 16 A. R. Ravishankara, *Science*, **276**, 1058 (1997).
- 17 A. Tabazadeh, M. L. Santee, M. Y. Danilin, H. C. Pumphrey, P. A. Newman, P. J. Hamill, and J. L. Mergenthaler,

*Science*, **288**, 1407 (2000).

- 18 D. Mackay and W. Y. Shiu, *J. Phys. Chem. Ref. Data*, **10**, 1175 (1981).
- 19 A. B. Ross, B. H. J. Bielski, G. V. Buxton, C. L. Greenstock, W. P. Helman, R. E. Huie, J. Grodkowski, P. Neta, and W. G. Mallard, "NDRL-NIST Solution Kinetics database: Ver. 3," National Institute of Standards and Technology, Gaithersburg, Maryland (1994).
- 20 W. B. Demore, S. P. Sander, D. M. Golden, R. F. Hampson, M. J. Kurylo, C. J. Howard, A. R. Ravishankara, C. E. Kolb, and M. J. Molina, "Chemical Kinetics and Photochemical Data for Use in Stratospheric Modeling Evaluation No-12, JPL Publication-97-4," Jet Propulsion Laboratory, Pasadena, CA (1997).
- 21 "Handbook of Photochemistry," ed by S. L. Murov, I. Carmichael, and G. L. Hug, MerceL Dekker, New York (1993), p. 293.
- 22 S. N. Guha, P. N. Moorthy, K. Kishore, D. B. Naik, and K. N. Rao, *Proc. Indian Acad. Sci., (Chem. Sci.)*, **99**, 261 (1987).
- 23 T. N. Das, *J. Phys. Chem. A*, **105**, 9142 (2001).
- 24 G. V. Buxton and C. R. Stuart, *J. Chem. Soc., Faraday Trans.*, **91**, 279 (1995).
- 25 N. C. Rothman, D. F. Dever, D. Garcia, and E. Grunwald, *J. Phys. Chem.*, **90**, 6464 (1986).
- 26 J. G. Calvert and J. N. Pitts, "Photochemistry," John Wiley and Sons, New York, (1965) p. 489.
- 27 D. A. Skoog, "Principles of Instrumental Analysis," 3rd ed, Saunder's College Publishing, Philadelphia, (1985), p. 185.
- 28 G. V. Buxton, C. L. Greenstock, W. P. Helman, and A. B. Ross, *J. Phys. Chem. Ref. Data*, **77**, 513 (1988).
- 29 D. Zehavi and J. Rabani, *J. Phys. Chem.*, **76**, 312 (1972).
- 30 M. Simic, P. Neta, and E. Hayon, *J. Phys. Chem.*, **73**, 3794 (1969).
- 31 "CRC Hand Book of Chemistry and Physics," ed by D.R. Lide, CRC Press, New York (1995), pp. 8-87.
- 32 Z. Zhang, R. D. Saini, M. J. Kurylo, and R. E. Huie, *Geophys. Res. Lett.*, **19**, 2413 (1992).